World Scientific
www.worldscientific.com

CARRIER–LATTICE RELAXATION FOR BROADENING EPR LINEWIDTH IN $Nd_{0.55}Sr_{0.45}MnO_3$

JIYU FAN[*,‖], XIYUAN ZHANG[*], WEI TONG[†], LEI ZHANG[†], WEICHUN ZHANG[*],
YAN ZHU[*], YANGGUANG SHI[*], DAZHI HU[*], BO HONG[‡], YAO YING[§],
LANGSHENG LING[†], LI PI[†,¶] and YUHENG ZHANG[†,¶]

[*]Department of Applied Physics,
Nanjing University of Aeronautics and Astronautics, Nanjing 210016, China
[†]High Magnetic Field Laboratory, Chinese Academy of Sciences, Hefei 230031, China
[‡]Department of Material Engineering, China Jiliang University, Hangzhou 310018, China
[§]Institute of Magnetic and Electronic Materials,
College of Chemical Engineering and Materials Science,
Zhejiang University of Technology, Hangzhou 310023, China
[¶]Hefei National Laboratory for Physical Sciences at the Microscale,
University of Science and Technology of China, Hefei 230026, China
[‖]jiyufan@nuaa.edu.cn

In this paper, we report the electron paramagnetic resonance (EPR) study of perovskite manganite $Nd_{0.55}Sr_{0.45}MnO_3$. Experimental data reveal that the EPR linewidth broadens with a quasilinear manner up to 480 K. The broadening of the EPR linewidth can be understood in terms of the shortening of carrier–lattice relaxation time due to the occurrence of strong carrier–phonon interactions. Two same activation energies obtained respectively from the temperature dependence of EPR intensity and resistivity indicate that the linewidth variation is correlated to the small polaron hopping. Therefore, the carrier–lattice coupling play a major role for deciding its magnetism in the present system.

Keywords: EPR; spin–phonon coupling; manganite.

1. Introduction

The rare-earth based manganites showing exotic properties such as colossal magnetoresistance, charge ordering, etc. have been the focus of extensive investigation not only for fundamental interest but also due to their potential applications.[1–8] Doped manganites $R_{1-x}A_xMnO_3$ (R = rare earth element, A = divalent alkaline earth element) have distorted perovskite structure. Due to strong electron–phonon coupling in manganites, it is recognized that the hopping electrons between Mn^{3+} and

[‖]Corresponding author.

Mn^{4+} show as polarons rather than "bare" e_g electrons.[9] More studies presented evidences that transport carriers in paramagnetic (PM) phase should be described as small polarons.[10–13] Besides the electronic detection of small polaron transport, electron paramagnetic resonance (EPR) has been also used to investigate its properties because EPR is an effective means to study the spin dynamics and magnetic correlation in doped perovskite manganites.

At present, the broadening PM resonance linewidth with temperature is a common observation in many doped manganites. However, its origin has not been fully understood. Main disputation focuses on two aspects, viz. ion–ion spin relaxation and carrier–lattice relaxation. Rettori *et al.* think that the broadening of PM resonance linewidth is associated with the spin–lattice interaction involving the one phonon process.[14] However, Shengelaya *et al.* proposed the polaron hopping contribution for PM linewidth as they investigated EPR of $La_{1-x}Ca_xMnO_3$.[15,16] They thought that the hopping rate of charge carriers limited the lifetime of the spin state which lead to the broadening of the EPR linewidth. Recently, the question has been revived by Huber,[17] who first proposed spin–spin exchange interaction for the contribution of linewidth.[18] According to Huber's approach, Rozenberg *et al.* found that the spin–spin relaxation is appropriate only for electron-doped and pristine manganite whereas the carrier–lattice relaxation plays key role in hole-doped manganite.[19] Therefore, in order to further clarify this issue, it is well worth investigating the linewidth variation and the polarons hopping contribution for EPR linewidth.

In this paper, we investigated the EPR of manganite $Nd_{0.55}Sr_{0.45}MnO_3$ which just lays at the boundary of ferromagnetic and charge ordering-antiferromagnetic phase. The obtained results show that there are strong carrier–lattice coupling in the PM region. Through the analysis of peak-to-peak linewidth ΔH_{pp} and double integrated intensities (DIN), we find that it is due to the carrier–lattice relaxation for the broadening of EPR linewidth in the present material.

2. Experiment

The polycrystalline $Nd_{0.55}Sr_{0.45}MnO_3$ sample was prepared by traditional solid-state reaction method. The detailed process has been reported in our previous report.[20] The structure and phase purity of the sample were checked by powder X-ray diffraction (XRD) using CuK_α radiation at room temperature. The XRD patterns prove that the sample is pure and a single-phase with orthorhombic structure. The EPR measurement of the powder sample was performed at selected temperatures using a Bruker EMX-plus model spectrometer with a heater operating at X-band frequencies ($\nu \approx 9.4$ GHz).

3. Results and Discussion

The perovskite manganite $Nd_{0.55}Sr_{0.45}MnO_3$ is a ferromagnetic (FM) oxide, where T_C is about 280 K. Its detailed magnetic structure has been reported in the previous
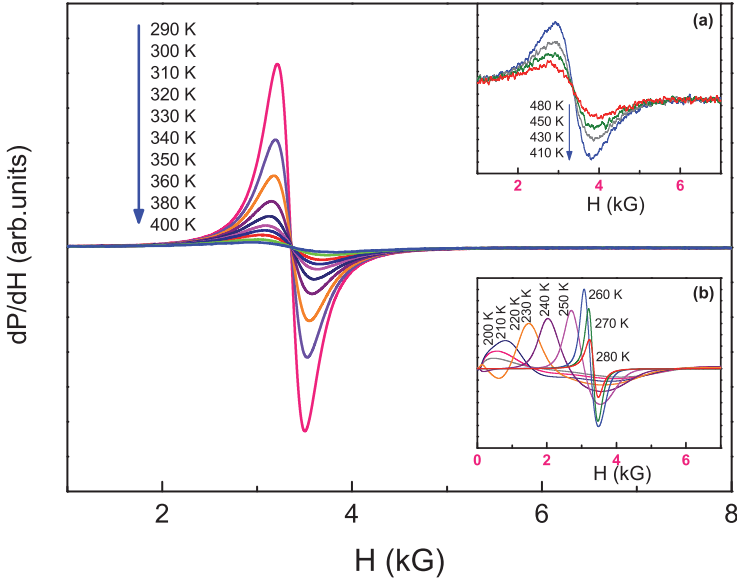
Fig. 1. (Color online) EPR spectrum of $Nd_{0.55}Sr_{0.45}MnO_3$ at temperatures of 290 K $\leq T \leq$ 400 K. Inset (a) and (b) show the spectrum for 410 K $\leq T \leq$ 480 K and for 200 K $\leq T \leq$ 280 K, respectively.

investigation.[21,22] In addition, the PM-FM phase transition has been recently found in the magnetic material $NdFe_{1-x}Ni_xO_3$.[23] Figure 1 shows some representative EPR spectra of $Nd_{0.55}Sr_{0.45}MnO_3$ at different temperatures. Above $T = 280$ K, a single resonance line with Lorentzian shape was observed. Below $T = 280$ K, as shown in inset of Fig. 1(b), a resonance peak gradually shifts into low field region and the strength of PM resonance decreases. At $T \leq 250$ K, the resonance lines had deviated from Lorentzian shape and shown a noticeable broadening. In general, the intensity of EPR resonance line is proportional to the total number of PM spins. Therefore, the decrease of resonance intensity indicates the decrease of PM ions at $T \leq 280$ K. For $Nd_{0.55}Sr_{0.45}MnO_3$, its PM-FM phase transition just occurs in ~ 280 K. The change of PM resonance shape is consistent with the PM-FM phase transition observed from magnetization measurement.

Figure 2 graphs the temperature dependence of effective g-factor. The g-factor reflects the intensity of spin–orbit coupling. For a free electron, the g-factor is close to 2. As an electron is in the atom, the g-factor will shift from 2 due to the spin–orbit coupling. Therefore, the determination of g value needs to take into account the local environment of the spin system. The effective g-factor can be calculated from the resonance field formula $g = h\nu/\mu_B H_{res}$ (h is the Planck constant; ν is the frequency of microwave; μ_B is the Bohr magnetor). Generally, the g-factor is around 2.00 as the sample in PM state.[24] As shown in Fig. 2, the g-factor has non-trivial variation at $T > 350$ K but shows a rapid increase at $T < 300$ K. In order to reflect
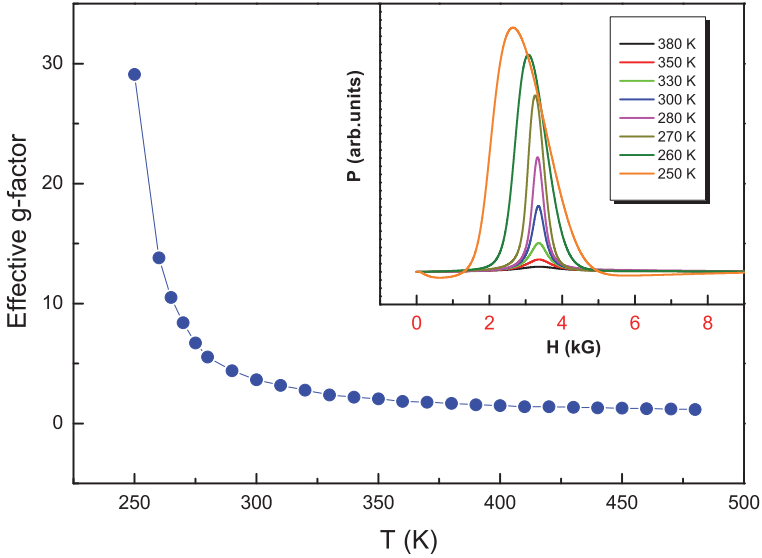
Fig. 2. (Color online) The effective g-factor as a function of temperature; the inset shows the absorption spectrum as a function of field at different temperatures.

this variation more clearly, the inset of Fig. 2 presents the absorption spectrum as a function of field in some typical temperatures cross T_C. Obviously, the resonance field H_{res} gradually shifts to low field regime as temperature decreases from 380 K to 250 K. The increase of g-factor is in agreement with the shift of absorption spectrum. However, we noticed that the g-factor of 350 K was 2.05 near to the $g \sim 2$ for a free electron but g-factor of 300 K had reached to 3.63 far from 2. On the other hand, the temperature of PM-FM phase transition of $Nd_{0.55}Sr_{0.45}MnO_3$ is 280 K. At $T = 300$ K, the system is in the PM state. Therefore, the large g-factor indicates that the increase of g-factor is strongly correlated to the change of spin–orbital coupling. The coupling between spin and orbital momentums can cause a local magnetic moments of Mn^{3+}/Mn^{4+} ions. Their interactions form some FM spin clusters which embeds in the background of PM phase. This phenomenon is generally recalled as "magnetic phase separation." In fact, the existence of phase separation has been found in the early investigation of $Nd_{0.55}Sr_{0.45}MnO_3$ (see Ref. 21) and testified in the recent pressure experiment in the similar material $Nd_{0.53}Sr_{0.47}MnO_3$.[25] Therefore, the additional spin–orbit coupling causes the orbital ordering, which changes the crystal field splitting and hence results in an increase of g-factor.

The temperature variations of the peak-to-peak linewidth ΔH_{pp}, as functions of temperature is shown in Fig. 3(a). Upon cooling from $T = 480$ K, ΔH_{pp} displays a narrow minimum at 300 K ($\simeq 1.1\ T_C$). The minimum is an universal feature and is analogous to that observed in the other doped manganite.[14,16,26–29] Generally, the broadening of ΔH_{pp} is due to the spin-related relaxation process. At present, the quasilinear increase of ΔH_{pp} above T_C can be understood with the following
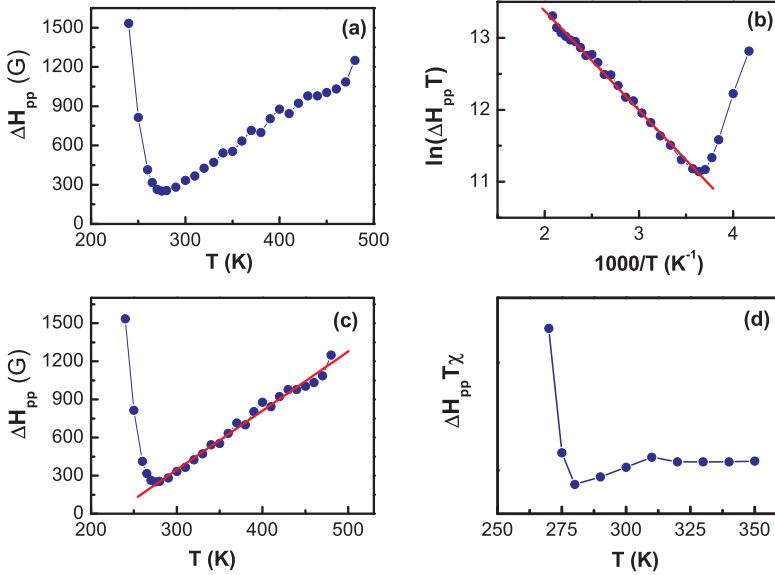
Fig. 3. (Color online) (a) The EPR linewidth ΔH_{pp} versus T. (b) The solid line represents the fit with formula of model (i). (c) The solid line represents the fit with formula of model (iii). (d) The temperature dependence of the product $\Delta H_{pp} T \chi$.

four mechanisms:

(i) the bottlenecked spin relaxation form an exchange interaction between Mn^{3+} and Mn^{4+} proposed by Shengelaya *et al.*,[15]

(ii) a spin-only relaxation proposed by Causa *et al.*,[30]

(iii) the combination of exchange narrowing spin–spin coupling and spin–lattice coupling proposed by Yuan *et al.*,[31]

(iv) a spin–phonon coupling proposed by Seehra *et al.*[32]

For model (i), we have not found the activated temperature dependence which is related to bottleneck mechanism. Moreover, according to model (i), the linewidth can be expressed with formula $\Delta H_{pp}(T) = \Delta H_0 + \frac{A}{T} \exp(-E_a/k_B T)$. We fitted the experimental linewidth ΔH_{pp} with it [see Fig. 3(b)]. However, the activation energy is deduced to be 119.2 meV, which is much larger than the activation energy $E_a = 72.4$ meV obtained from resistivity curve (see the following discussion). So, model (i) is not valid for the present $Nd_{0.55}Sr_{0.45}MnO_3$. Such an inconsistency of temperature-dependence of PM ΔH_{pp} and resistivity ρ was also found in $Pr_{0.7}Ca_{0.15}Ba_{0.15}MnO_3$ by Ulyanov *et al.*[33] For model (ii), an obvious deviation from the quasilinear temperature dependence of $\Delta H_{pp}(T/T_C)$ versus $\Delta H_{pp}(\infty)$ was observed in our sample (not shown here). Therefore, model (ii) is no valid as well. According to model (iii), the ΔH_{pp} can be describe with

$$\Delta H_{pp} = \Delta H_{pp,min} + b(T - T_{min}). \tag{1}$$

The first term $\Delta H_{\mathrm{pp,min}}$ is related to the exchange narrowing spin–spin coupling while the second term $b(T - T_{\mathrm{min}})$ is due to the spin–lattice coupling. By using this model, we deduced the $\Delta H_{\mathrm{pp,min}}$ to be 235 Gauss which is very near to our experimental 250 Gauss (see Fig. 3(c)). Therefore, model (iii) seems to be adapted to the system. According to model (iv), the linear dependence of linewidth in manganites is attributed to critical and non-critical contributions. Both contributions for the linewidth can be written with

$$\Delta H_{\mathrm{pp}}(T) = \frac{\hbar[c + f(\epsilon)]}{g\mu_{\mathrm{B}} T \chi_0}\,, \tag{2}$$

where $f(\epsilon)$ is the critical contribution to ΔH_{pp} from spin–spin coupling, which is significant only for $\epsilon = (T - T_C)/T_C \leq 0.1$ and c is non-critical contribution to ΔH_{pp} from spin–phonon interactions for $T \gg T_C$. If there is no contribution to the linewidth from spin–phonon (vibrations of the lattice) interactions, the product $\Delta H_{\mathrm{pp}} T \chi$ should be a temperature independent constant at $T \gg T_C$. Thus, Eq. (2) can be simplified as

$$\Delta H_{\mathrm{pp}}(T) = \Delta H_{\mathrm{pp}}(\infty) \frac{C}{T\chi}\,, \tag{3}$$

where C/T is the single ion susceptibility, χ is the measured PM susceptibility and $\Delta H_{\mathrm{pp}}(\infty)$ is the linewidth expected at temperature high enough. Figure 3(d) shows the product $\Delta H_{\mathrm{pp}} T \chi$ as a function of temperature above T_C. Obviously, the value of $\Delta H_{\mathrm{pp}} T \chi$ is a function of temperature, indicating that there are spin–phonon interactions in the system. In fact, we find that models (iii) and (iv) have some similarities and both of them describe the same contribution of spin–phonon interactions to the broadening linewidth. Generally, in conventional magnetic materials, spin relaxation mainly depends on the relaxation times between local moments and itinerated electron, namely, carrier–lattice spin relaxation. The exchange interaction between local moments and conduction electrons results in a temperature-linear contribution to the total EPR linewidth. For the present $Nd_{0.55}Sr_{0.45}MnO_3$ system, the main local magnetic moments are from Mn^{3+} and Mn^{4+} ions. The conduction electron's spin is from e_g electrons or polaron due to the existence of intense electron–phonon coupling. In PM region, the rise of temperature intensifies the lattice vibration. Therefore, the spin–phonon interaction effectively decreases the spin–lattice relaxation time and consequently results in the broadening of the EPR linewidth.

Taking into account the intense spin–phonon coupling in the present sample, we have to clarify the contribution of small polaron for the ΔH_{pp} variation. In PM regime, the conductivity of hole-doped manganites is generally dominated by the adiabatic small polaron hopping model. In Fig. 4(a), we fitted the experimental resistivity curve (ρ versus T) with the small polaron hopping model $\rho = \rho_0 T \exp(E_a/k_{\mathrm{B}}T)$, where E_a is the activation energy for small polaron hopping. From the fitting results, we obtained the activation energy $E_a = 72.4$ meV. In the previous investigations of $Nd_{0.6}Sr_{0.4}MnO_3$ and $Nd_{0.5}Sr_{0.5}MnO_3$ by Angappane
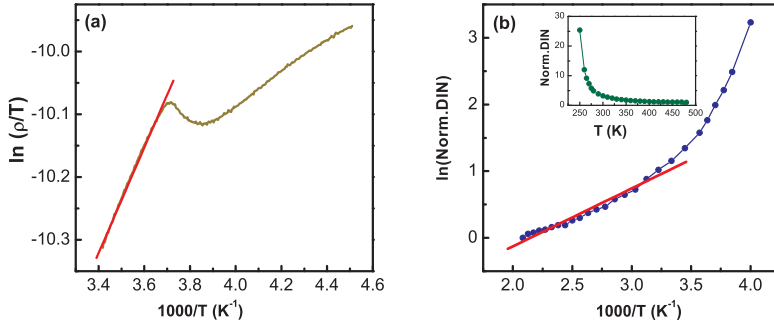
Fig. 4. (Color online) (a) $\ln(\rho/T)$ shows as a function of inverse temperatures (bottom axis) and the solid lines denotes the fit with the small polaron hopping model. (b) Arrhenius plots of DIN and the solid line represents the fit with Eq. (4) (the inset represents the ESR intensity I_{EPR} versus T).

et al., the activation energies were reported to be $E_a = 100$ meV and 60 meV, respectively.[34] The present sample $Nd_{0.55}Sr_{0.45}MnO_3$ is in the middle of them. Therefore, the obtained activation energy of $E_a = 72.4$ meV should be reasonable and credible. In order to further testify whether the small polaron hopping contributes to the broadening linewidth, we have studied the intensity of EPR spectra which is related to all magnetic ions contribution to the resonant entities. Two different numerical analysis methods are used to calculate the intensity of EPR spectra. One is double integration of the spectra (dP/dH) and the other is calculation of the area of production $\Delta H_{\text{pp}}^2 Y'$, where $2Y'$ is the peak-to-peak derivative amplitude. Both methods gave similar results but the first one provided better accuracy for absolute values. Therefore, we use the double integrated intensities (DIN) to analyze the intensity of EPR spectra. The inset of Fig. 4(b) presents the results of normalized DIN. Similar to the change of g-factor, the DIN increases sharply at $T < 300$ K characteristic for the developing FM order. The DIN of PM region is usually described by the Arrhenius law:[26,30]

$$\text{DIN}(T) = I_0 \exp(E_a/k_B T), \qquad (4)$$

where E_a is the activation energy for dissociation of the PM spin clusters. As shown in Fig. 4(b), the activation energy was deduced to be 75.1 meV, which is very close to the $E_a = 72.4$ meV deduced from the temperature dependence of the resistivity curve. $Nd_{0.55}Sr_{0.45}MnO_3$ is a special kind of ferromagnetic materials, which is near to the half-doping charge ordering $Nd_{0.5}Sr_{0.5}MnO_3$. Therefore, its spin–lattice and spin–orbital coupling is so strong that the carrier shows as the polarons rather than bare electron. In addition, the manganites widely shows inhomogeneity.[35–37] Thus, above T_C, there may be some spin clusters to appear in PM state. As the temperature tends to T_C, the spin–orbital coupling not only forms the ferromagnetic coupling at inner part of cluster, but also causes the ferromagnetic correlation among the adjacent clusters.[38] For the carrier transport, the local ferromagnetic

interaction can help its delocalization. On the other hand, the rise of temperature enhances the thermal vibration of lattice. Therefore, the intense spin–phonon interaction promotes the development of polarons. In this case, the polarons hopping becomes easy and the spin–lattice relaxation time shortens. Consequently, the broadening of linewidth was observed in PM regime during the EPR measurement.

4. Conclusion

In summary, we have measured the EPR spectra of $Nd_{0.55}Sr_{0.45}MnO_3$ at different temperatures. A quasilinear increase of EPR linewidth has been maintained from T_C up to 480 K. The broadening EPR linewidth originates from the increase of carrier–lattice relaxation rate. The similar values of the activation energy obtained from two different methods indicates the existence of strong spin–phonon interactions and spin clusters correlation in the present system.

Acknowledgment

References

1. R. von Helmolt, J. Wecker, B. Holzapfel, L. Schultz and K. Samwer, *Phys. Rev. Lett.* **71** (1993) 2331.
2. S. Jin, T. H. Tiefel, M. McCormack, R. A. Fastnacht, R. Ramesh and L. H. Chen, *Science* **264** (1994) 413.
3. K. Chahara, T. Ohno, M. Kassai and Y. Kozono, *Appl. Phys. Lett.* **63** (1993) 1990.
4. A. Moreo, S. Yunoki and E. Dagotto, *Science* **283** (1999) 2034.
5. M. Tokunaga, N. Miura, Y. Tomioka and Y. Tokura, *Phys. Rev.* **57** (1998) 5259.
6. C. Kapusta, P. C. Riedi, M. Sikora and M. R. Ibarra, *Phys. Rev. Lett.* **84** (2000) 4216.
7. S. Dong, R. Yu, J.-M. Liu and E. Dagotto, *Phys. Rev. Lett.* **103** (2009) 107204.
8. H.-L. Yang, Y.-W. Liu and R.-W. Li, *SPIN* **2** (2012) 1230004.
9. A. J. Millis, P. B. Littlewood and B. I. Shraiman, *Phys. Rev. Lett.* **74** (1995) 5144.
10. M. Jaime, M. B. Salamon, M. Rubinstein, R. E. Treece, J. S. Horwitz and D. B. Chrisey, *Phys. Rev. B* **54** (1996) 11914.
11. J. M. De Teresa, K. Dörr, K. H. Müller, L. Schultz and R. I. Chakalova, *Phys. Rev. B* **58** (1998) R5928.
12. S. Fratini and S. Ciuchi, *Phys. Rev. Lett.* **91** (2003) 256403.
13. N. Mannella, A. Rosenhahn, C. H. Booth, S. Marchesini, B. S. Mun, S.-H. Yang, K. Ibrahim, Y. Tomioka and C. S. Fadley, *Phys. Rev. Lett.* **92** (2004) 166401.
14. C. Rettori, D. Rao, J. Singley, D. Kidwell, S. B. Oseroff, M. T. Causa, J. J. Neumeier, K. J. McClellan, S.-W. Cheong and S. Schultz, *Phys. Rev. B* **55** (1997) 3083.
15. A. Shengelaya, G.-M. Zhao, H. Keller and K. A. Müller, *Phys. Rev. Lett.* **77** (1996) 5296.
16. A. Shengelaya, G.-M. Zhao, H. Keller and K. A. Müller, *Phys. Rev. B* **61** (2000) 5888.

17. D. L. Huber, *J. Magn. Magn. Mater.* **324** (2012) 2113.

18. D. L. Huber, G. Alejandro, A. Caneiro, M. T. Causa, F. Prado, M. Tovar and S. B. Oseroff, *Phys. Rev. B* **60** (1999) 12155.

19. M. Auslender, E. Rozenberg, A. I. Shames and Ya. M. Mukovskii, *J. Appl. Phys.* **113** (2013) 17D705.

20. J.-Y. Fan, L. Pi, L. Zhang, W. Tong, L.-S. Ling, B. Hong, Y.-G. Shi, W.-C. Zhang, D. Lu and Y.-H. Zhang, *Appl. Phys. Lett.* **98** (2011) 072508.

21. C.-W. Cui, T. A. Tyson, Z.-Q. Chen and Z. Zhong, *Phys. Rev. B* **68** (2003) 214417.

22. J.-Y. Fan, L. Pi, Y. He, L.-S. Ling, J.-X. Dai and Y.-H. Zhang, *J. Appl. Phys.* **101** (2007) 123910.

23. A. Bashir, M. Ikram and R. Kumar, *Mod. Phys. Lett. B* **25** (2011) 2439.

24. J.-Y. Fan, W. Tong, L. Zhang, Y.-G. Shi, Y. Zhu, D.-Z. Hu, W.-C. Zhang, Y. Ying, L.-S. Ling, L. Pi and Y.-H. Zhang, *Phys. Status Solidi B* **249** (2012) 1634.

25. M. Baldini, Y. Ding, S. Wang, Y. Lin, C. A. Tulk, A. M. dos Santos, J. F. Mitchell, D. Haskel and W. L. Mao, *Phys. Rev. B* **86** (2012) 094407.

26. A. I. Shames, E. Rozenberg, W. H. McCarroll, M. Greenblatt and G. Gorodetsky, *Phys. Rev. B* **64** (2001) 172401.

27. A. I. Shames, E. Rozenberg, G. Gorodetsky and Ya. M. Mukovskii, *Phys. Rev. B* **68** (2003) 174402.

28. S. B. Oseroff, M. Torikachvili, J. Singley, S. Ali, S.-W. Cheong and S. Schultz, *Phys. Rev. B* **53** (1996) 6521.

29. J. Q. Li and S. L. Yuan, *Solid State Commun.* **134** (2005) 295.

30. M. T. Causa, M. Tovar, A. Caneiro, F. Prado, G. Ibañez, C. A. Ramos, A. Butera, B. Alascio, X. Obradors, S. Piñol, F. Rivadulla, C. Vázquez-Vázquez, M. A. López-Quintela, J. Rivas, Y. Tokura and S. B. Oseroff, *Phys. Rev. B* **58** (1998) 3233.

31. S. L. Yuan, G. Li, Y. Jiang, J. Q. Li, X. Y. Zeng, Y. P. Yang, Z. Huang and S. Z. Jin, *J. Phys.: Condens. Matter* **12** (2000) L109.

32. M. S. Seehra, M. M. Ibrahim, V. Suresh Babu and G. Srinivasan, *J. Phys.: Condens. Matter* **8** (1996) 11283.

33. A. N. Ulyanov, H. D. Quang, N. E. Pismenova, S. C. Yu and G. G. Levchenko, *Solid State Commun.* **152** (2012) 1556.

34. S. Angappane, G. Rangarajan and K. Sethupathi, *J. Appl. Phys.* **93** (2003) 8334.

35. J. M. De Teresa, M. R. Ibarra, P. A. Algarabel, C. Ritter, C. Marquina, J. Blasco, J. Garcia, A. del Moral and Z. Arnold, *Nature (London)* **386** (1997) 256.

36. M. Uehara, S. Mori, C. H. Chen and S.-W. Cheong, *Nature (London)* **399** (1999) 560.

37. J. Burgy, M. Mayr, V. Martin-Mayor, A. Moreo and E. Dagotto, *Phys. Rev. Lett.* **87** (2001) 277202.

38. R. Yu, S. Dong, C. Şen, G. Alvarez and E. Dagotto, *Phys. Rev. B* **77** (2008) 214434.